INTERNATIONAL CENTRE FOR THE ... SCIENCES
LIBRARY

INTERNATIONAL ATOMIC ENERGY AGENCY
UNITED NATIONS EDUCATIONAL, SCIENTIFIC AND CULTURAL ORGANIZATION

INTERNATIONAL CENTRE FOR THEORETICAL PHYSICS
34100 TRIESTE (ITALY) - P.O.B. 586 - MIRAMARE - STRADA COSTIERA 11 - TELEPHONE: 2240-1
CABLE: CENTRATOM - TELEX 460392-I

SMR/208 - 39

SPRING COLLEGE IN MATERIALS SCIENCE

ON

"METALLIC MATERIALS"

(11 May - 19 June 1987)

SURFACE TREATMENT AND COATINGS OF MATERIALS
(Part III)

R. BULLOUGH
Materials Development Division
B552 Harwell Laboratory
Oxfordshire OX11 ORA
U.K.

These are preliminary lecture notes, intended only for distribution to participants.

LECTURE 3

THIN FILM PROPERTIES

Abstract

Fundamental to the successful exploitation of coatings in advanced applications is a detailed knowledge of the properties of thin films. Many examples exist to demonstrate that the properties of thin films are not the same as those of their bulk material counterparts; for example, the Young's modulus of a ceramic coating can be an order of magnitude lower than that of its bulk counterpart. In this lecture, the properties of thin films will be addressed from both an experimental and theoretical viewpoint.

Slide 1 — TITLE SLIDE : Thin Film Properties

Slide 2 — Many examples exist where coatings are deposited onto engineering components which operate in adverse conditions. Therefore, a knowledge of coating properties is important to assure the life of the coated material.

Slide 3 — This slide gives quantitative data on the operating advantages to be gained from using titanium nitride on coating drills. The coating speed can be significantly increased and/or the rate of coating can be increased.

Slide 4 — Typical examples of increases in cutting tool life as a result of using titanium nitride are shown in this slide.

Slide 5 — One of the most important properties is coating hardness and the basic requirements for modelling the hardness of thin films and coatings are given in this slide.

Slide 6 — One of the first attempts at modelling hardness was the area law of mixtures where the composite hardness of the material is assumed to be the area weighted advantage of the hardnesses of the substrate and surface film.

Slide 7 — A more realistic description of the deformation behaviour occurring beneath a hardness indenter is one of a deforming volume as shown in this slide.

Slide 8 — It is important, however, to take account of adhesion in these systems and the volume law of mixture has been modified by incorporation of an interface parameter termed χ.

Slide 9 — This interface parameter modifies the deforming volume in the substrate to take account of the constraint imposed by the adhesion of the coating to the substrate.

Slide 10 — It was found empirically that the interface parameter χ was a linear function of the relative deforming volumes in the coating and the substrate.

Slide 11 — The results which are obtained from hardness modelling are presented in this slide. Line 1 is the hardness data of uncoated material, line 2 is the calculated hardness of an infinitely thick coating and line 3 is the computed fit to the experimental data by using the volume law of mixtures.

Slide 12 — In most materials the description of the deforming volumes in terms of an expanding spherical cavity is quite valid and this is illustrated in Figure A of this slide. However, in softer materials, one observes surface directed displacements and there is a need to modify the model to accommodate such effects.

Slide 13 — For titanium nitride coatings deposited onto stainless steel, these surface directed displacements cause ring cracking which is illustrated in Figure A. For a similar coating deposited onto a tool steel, then the description in terms of an expanding spherical cavity is more valid.

Slides 14/15 — The growth morphology of PVD coatings has been illustrated in the lecture "Microstructures" and the intercrystallite boundaries lie normal to the coating-substrate interface. This leads to unusual hardness anisotropy in these materials. Testing the columnar units end-on gives a high hardness value since neighbouring crystallites impose a constraint on deformation. In contrast, testing in a sideways direction, the crystallites usually slide past one another giving a lower hardness value.

Slide 16 — Clearly, hardness in orientation 'C' is much higher than in orientations 'A' and 'B' as a result of these microstructural effects.

Slide 17 — A prerequisite for a hard coating is that the intercolumnar boundaries are strong and interactive. If the boundaries are weak as in 'A', then a low hardness value will result, whilst in 'B' the dense microstructure guarantees a high hardness.

Slide 18 — The hardness of PVD titanium nitride increases with substrate bias voltage which can be equated to the density of the volume.

Slide 19 — The open boundaries in an unbiased microstructure are clearly seen in micrograph 'A' and these obviously will result in limited load support when compared with the dense high bias microstructure shown in 'B'.

Slide 20 — The improvement in load support offered by a dense microstructure is illustrated in this slide. Hardness impressions at the same load are obviously larger in the case of an unbiased microstructure since substrate effects become more important in this case.

Slide 21 — The properties of the coating can be changed significantly by the process parameters. For example, the microhardness of titanium carbide varies dramatically with substrate temperature. As the substrate temperature increases, dense columnar crystallites are formed which lead to the observation of higher hardness.

Slide 22 — Similarly, the substrate temperature during the deposition of silicon carbide films can affect both the hardness and the density of the film as we have seen schematically in previous slides on microstructure.

Slide 23 — The hardness of wear-resistant coatings is due to two factors: one is the very fine grain size established in the coatings during growth as illustrated by this TEM micrograph.

Slide 24 — The second, and perhaps less important, hardening mechanism is the defect density which exists in these coatings. Transmission electron microscopy shows the presence of a high density of defects.

Slide 25 — The relative contributions to coating hardness by these two mechanisms is illustrated in this slide. Clearly, grain size effects appear to dominate hardness.

Slide 26 — A method of measuring adhesion in these hard ceramic coated coating systems is the scratch test and this slide illustrates the importance of three factors in determining the so-called critical load for coating detachment.

Slide 27 — Earlier in the talk I described how the deforming volume of coating and substrate depend on the ratio modulus divided by hardness. For soft substrates, the stresses introduced by mismatch in deforming volumes give rise to a low value of critical load. When deforming volumes become more equal in coating and substrate, the value of L_c increases.

Slides 28/29 — It is possible to characterise the various modes of failure in the scratch test and these are illustrated in this slide. These failure modes can be clearly identified in real systems.

Slide 30 — INTERIM SUMMARY SLIDE

We have learned so far that advanced properties can be conferred onto industrially important components by the use of coatings. The microstructure of the coating critically affects the properties, for example, hardness, and this can be well modelled.

Slide 31 — Another industrially important application for coatings where advanced properties are required is via the use of ceramics in diesel engines, as illustrated in this slide, and zirconia coatings on diesel engine exhaust valves.

Slide 32 — One property which is crucial to the satisfactory performance of the coating is its mechanical strength. Unless the coating can withstand the stresses of the combustion chamber, then the advanced properties, like low thermal conductivity, will not be realised. This slide shows that the fracture stress of yttria stabilised zirconia is also affected by the concentration of yttria in the zirconia. Additionally, it should be noted that because the coating contains porosity and microcracks, it is impossible to define a single value for the fracture stress. It is necessary to think in terms of a probability of failure distribution function.

Slide 33

Typical data for the fracture strength and Young's modulus of ceramic coatings is presented in this slide. It is important to note that different processing routes can affect the properties produced. It should also be noted that the parameter known as the viable modulus is a measure of the extent of the statistical variation of the fracture stress. It is important to aim for a value for this modulus of approximately 20 in order to obtain reliable performance.

Slide 34

The properties of the as deposited coating can be modified by relatively straightforward heat treatment steps. For example, heat treating a zirconia coating at 1,000°C for fourteen days produces a significant increase in the fracture stress distribution.

Slide 35

A major use for thin films in the glass industry is to modify the optical properties of the surface. This is vividly illustrated in this slide. In physical terms the surface of the glass must be able to reflect a significant portion of the infra-red radiation falling onto the glass as shown in this slide showing transmission of light v. incident wave length.

Slide 36

In order to achieve this condition of selective heat reflection and light transmission, it is possible to deposit a multilayer coating comprising materials such as aluminium, alumina, molybdenum and alumina. This slide shows the spectral response of such a material.

Slide 37

This slide shows that it is possible to achieve a high degree of transmission selectivity as a result of using, for example, titania-copper-titania or titania-silver-titania multilayer coatings.

Slide 38

Moreover, in the coating process it is possible to vary the partial pressure of the oxygen in the reaction chamber to modify both the refractive and absorption indices of the surface of the glass.

Slide 39

Finally, as a note of general caution, it is important to remember that the properties of thin films may be significantly better than those of the bulk material as illustrated in this slide which is a plot of the microhardness of ceramic materials v. temperature for both bulk and thin film materials.

Slide 40

SUMMARY SLIDE

The main points to note from this lecture are that the properties of thin films can be different to bulk materials. It is possible to model properties quite accurately. It is necessary to measure the properties of ceramic coatings to establish their suitability for harsh applications. The properties of surfaces can be very precisely controlled as in the case of optical coatings.

THIN FILM PROPERTIES

Coatings

[illegible]

[illegible]

[illegible]

[illegible]

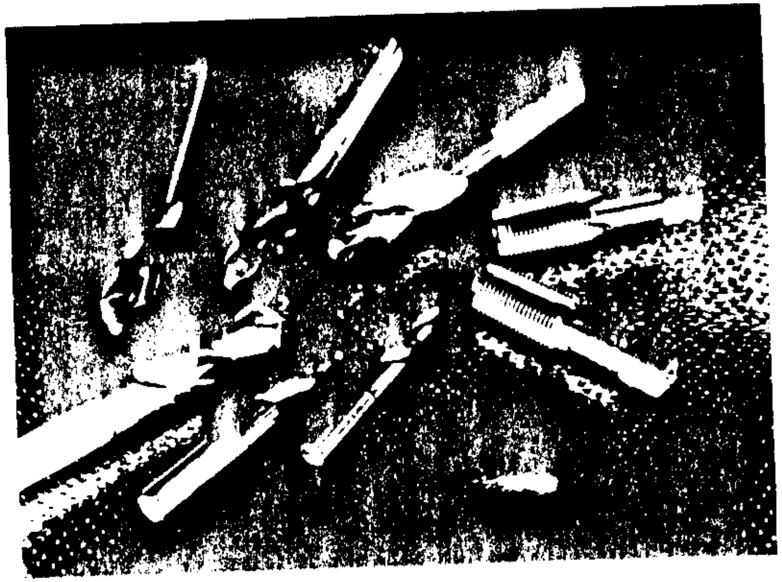

Yellow Ti Al [illegible] cutting tools

[illegible] | [illegible] knowledge of coating

[illegible] | [illegible] metal

LECTURE 3 : SLIDE 3

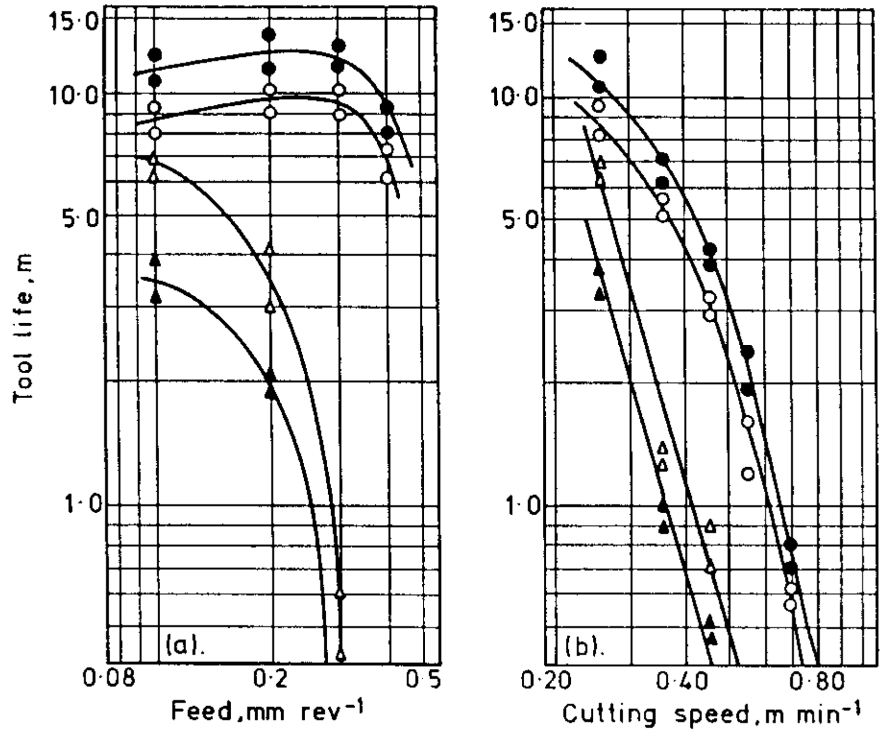

▲ Uncoated drill ● Balinit coated drill (new) TiN

△ Nitrided drill ○ Balinit coated drill (reground) TiN

Workpiece: plates made of 42CrMo4 (AISI 4140) tempered to 1000 MN m^{-2}, blind hole, 16 mm drilling depth

Test tool: Balinit coated drill, DIN 338, dia. 8 mm

Cooling by emulsion 1:20

Criterion for determining tool life: constant squeal

LECTURE 3 : SLIDE 4

TYPICAL INCREASES IN LIFE FOR SIP-TiN-COATED STEEL CUTTING TOOLS

Tool	Increase in Life
End mills	x 5
Shear blades	x 3
Parting-off tools	x 3.5
Gear shapers	x 2.5
Twist drills	x 10
Thread cutting dies	x 3
Monoblock hobs	x 3

BASIC REQUIREMENTS FOR MODELLING THE HARDNESS OF THIN FILMS & COATINGS

1 Want valid prediction over as large a range of indent sizes as possible for coating thicknesses of interest (e.g. 1-10μm for PVD TiN)

2 Applicable to a wide range of coating-substrate systems

3 Need to partition substrate & coating hardness contributions

   usually apply geometrical description of deformation process leading to a law-of-mixtures approach

4 Need to incorporate any indentation size effects in substrate or coating

5 Need to assume coating is homogeneous

AREA LAW-OF-MIXTURES

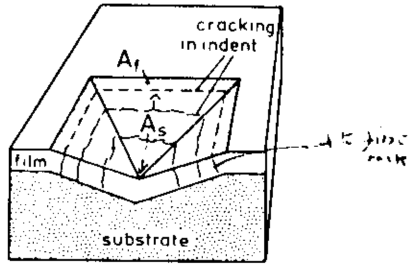

$A = A_s + A_f$

$$H_c = \frac{A_s}{A} H_s + \frac{A_f}{A} H_f$$

Early attempts:

Only works in limited cases eg Cr on Steel

VOLUME LAW-OF-MIXTURES

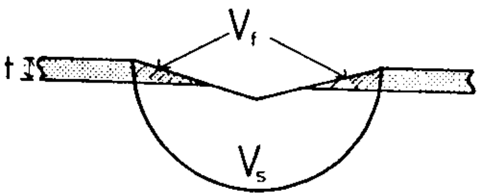

$$H_c = \frac{V_s}{V} H_s + \frac{V_s}{V} H_f$$ ← Fitted Andrews SiO₂ a glass.

Later attempts: Calc. relative deforming volume. Assume same modulus in coat & substrate.

Doesn't work in relatively systems.

MODIFIED VOLUME LAW-OF-MIXTURES

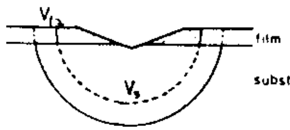

$\frac{E_f}{H_f} < \frac{E_s}{H_s}$

Effect of [illegible] E [illegible]

This factor influences the directionality

$$H_c = \frac{\chi^3 V_s}{V} H_s + \frac{V_f}{V} H_f \qquad H_f > H_s$$

where.

H_s, H_f incorporates a Meyer type ISE law, $H = ad^{m-2}$ — recognition that Hardness for ceramic is not a genuine material parameter.

V_s, V_f are calculated using the plastic zone radius given by $\frac{b}{a} \propto (E/H)^n$, $n = 1/3 - 1/2$.

χ is a plastic zone mismatch parameter and accounts for constraint of the softer substrate by the harder coating

$$\chi^3 \propto \left(\frac{E_f H_s}{H_f E_s} \right)^{1/2}$$

Evolved from Law of Mixtures to recent NONLINEAR DEP.

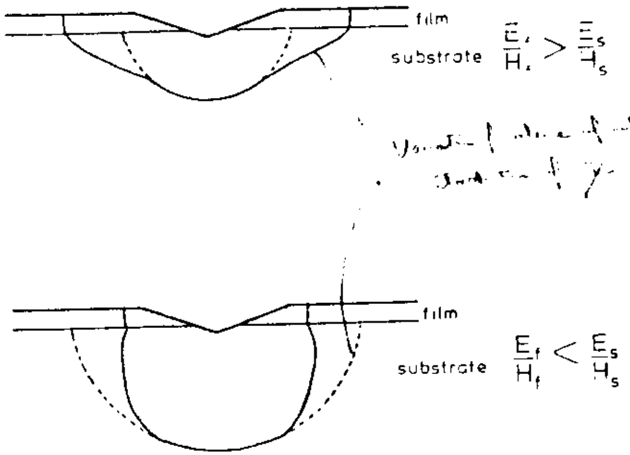

$x \gg 1$

$x < 1$

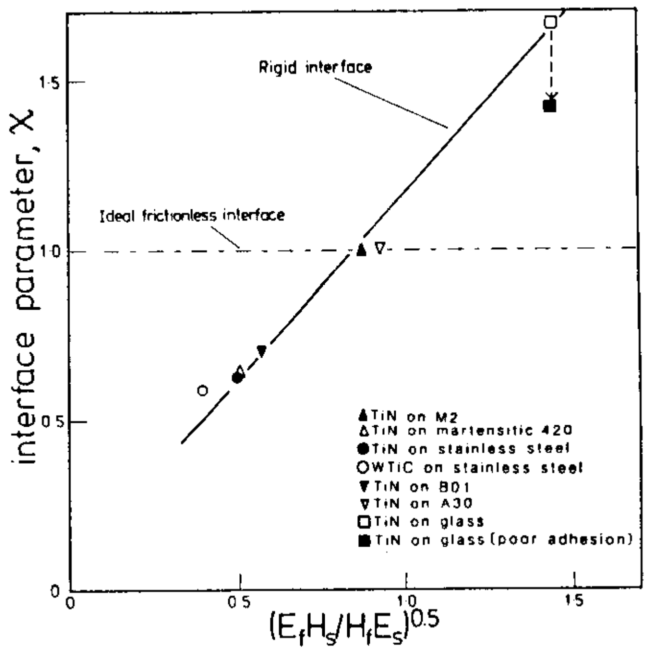

Experimentally found

TiN on whole range of substrates.

Now claim that $H_{composite}$ can be deduced from knowledge of H_s, H_f, E_s, E_f.

If film thickness is known then the procedure gives measure of film hardness when a coating

LECTURE 3 : SLIDE 11

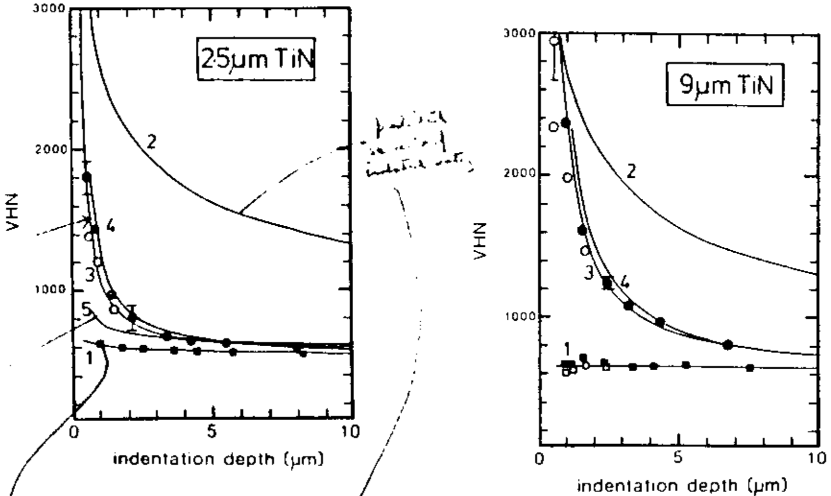

such that (2 + 1) yield (3 ~~4~~)
i.e. VOL. LAW + X

1, 5 is area law of mixtures
(power fit to data)

4 area law with indentation size effect included.
'Rebalance of Hardness' (Meyer Law) – accounted for ceramic coatings
As load decreases Hardness

Works o.k. for TiN on hard substrates (Tool steel)

Does not work on soft substrates such as S.S. – Then you need VOL LAW w. X etc.

This method appears to [illegible]

LECTURE 3 : SLIDE 12

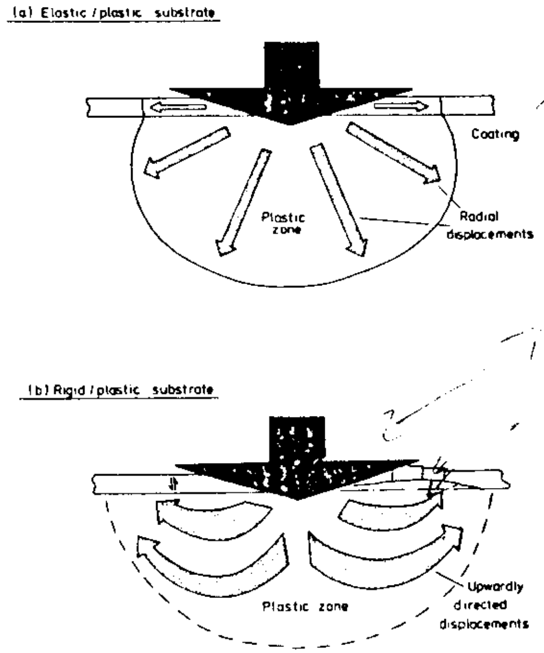

Expanding spherical cavity model – all displacements are radial. Surface directed displacements can crack the coating.

Probably these coating cracking effects should be included.

LECTURE 3 : SLIDE 13

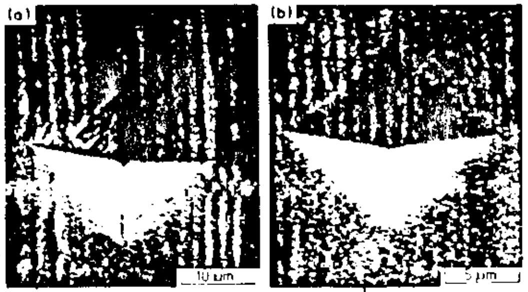

LECTURE 3 : SLIDE 14

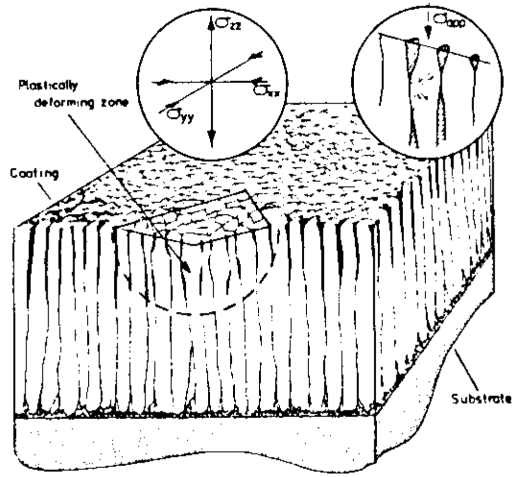

PVD

Highly anisotropic hardness

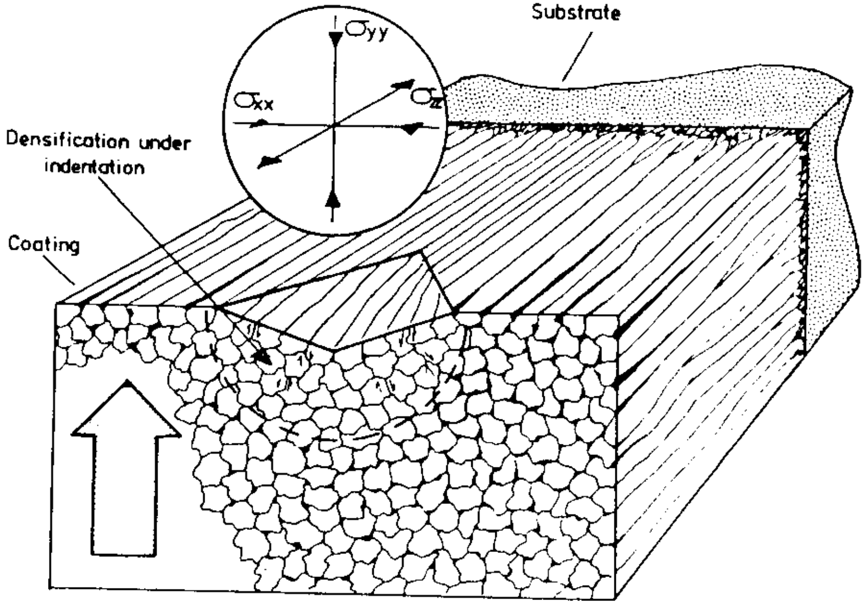

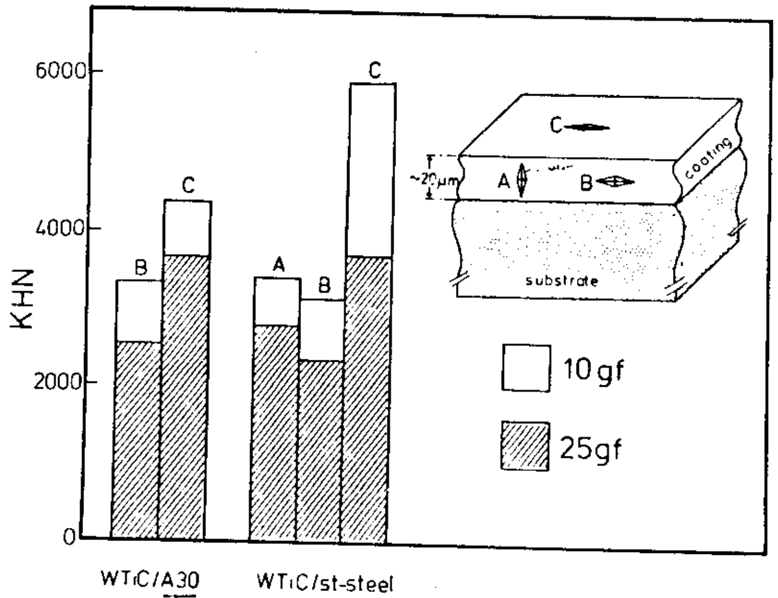

Note in CVD with equi axed microstructure we don't get this anisotropy! H

LECTURE 3 : SLIDE 17

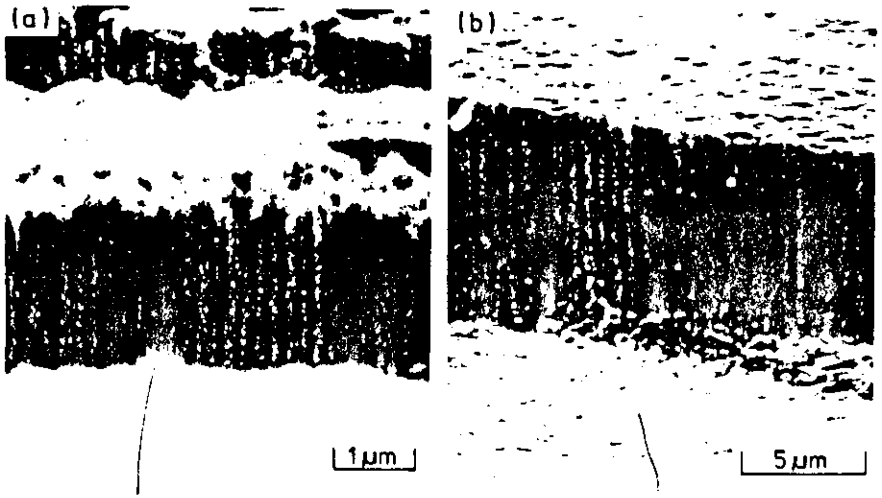

BIAS
Effect

LECTURE 3 : SLIDE 18

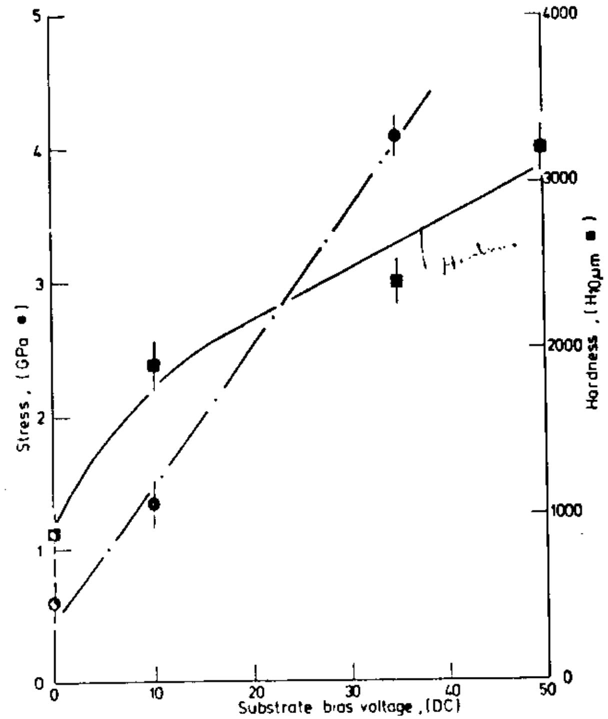

TiN on SS.

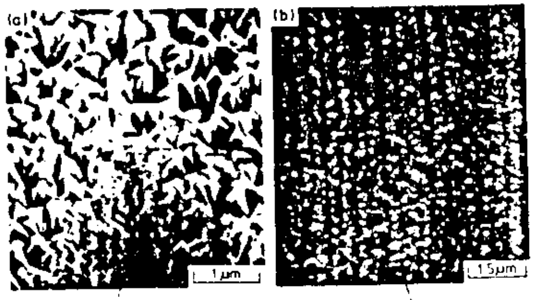

unbiased

biased

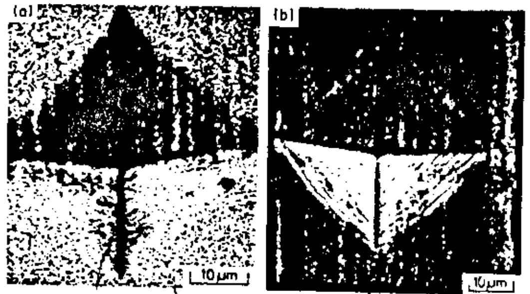

unbiased

biased

High load

LECTURE 3 : SLIDE 21

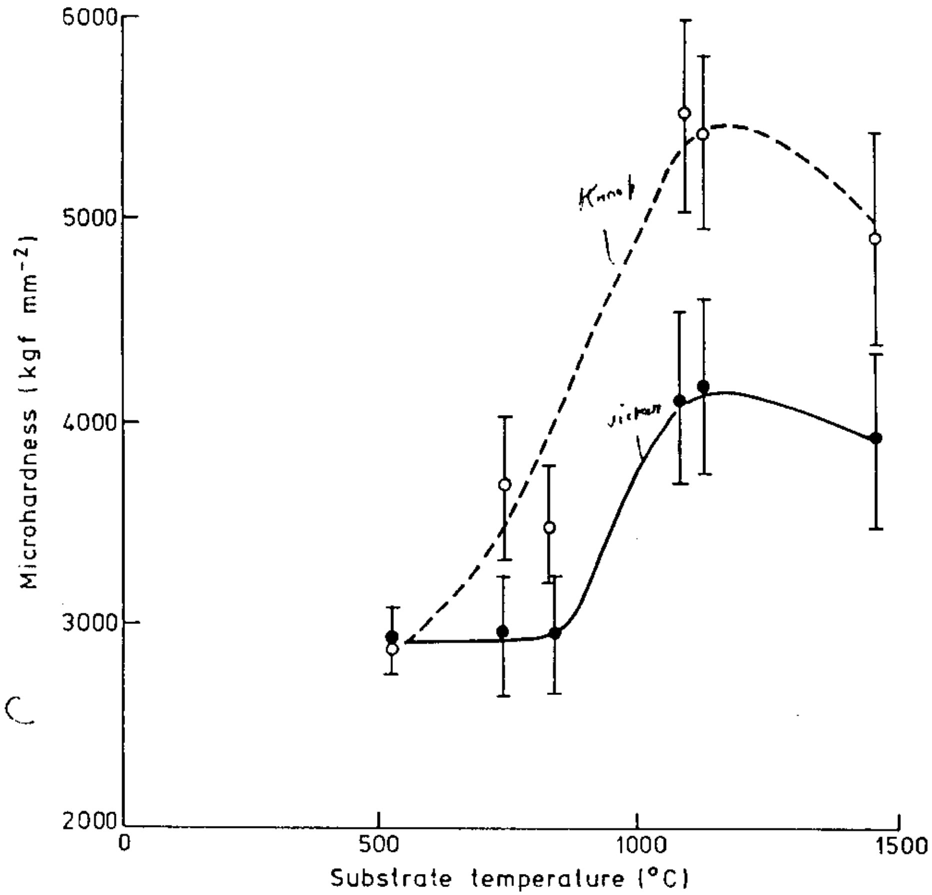

Ti C

Mo ?

Effect of Process Parameters

Columnar grains are breaking → tend to equiaxed

Diffusion processes coming in

Bunshah

LECTURE 3 : SLIDE 22

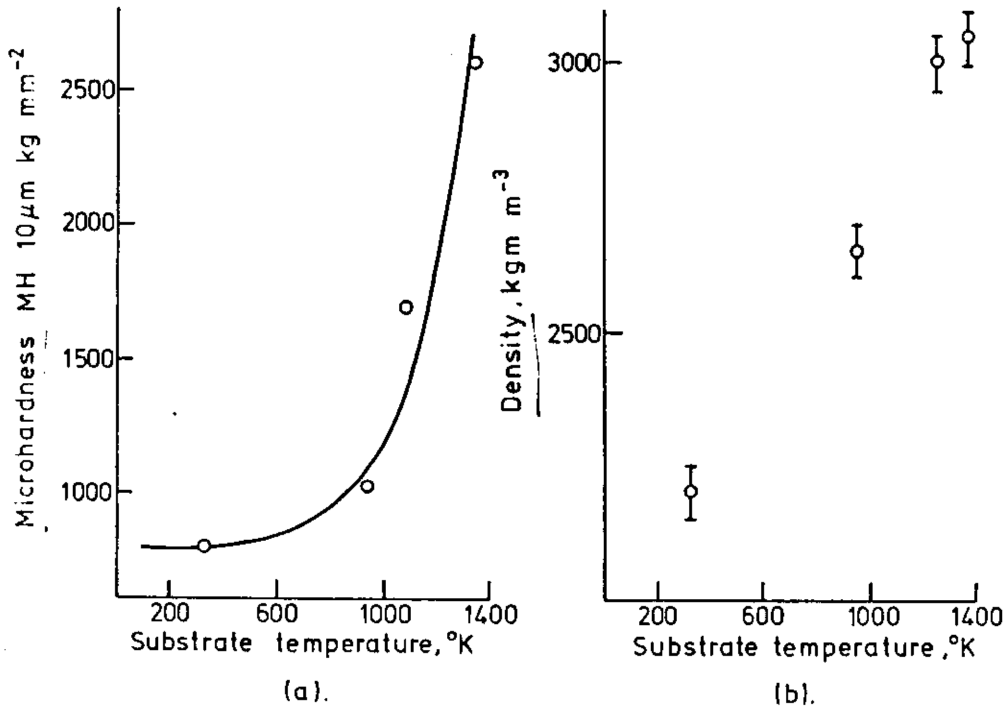

The effect of substrate temperature on (a). microhardness and (b). density of β SiC films

PACVD

LINGER

TiN

LECTURE 3 : SLIDE 23

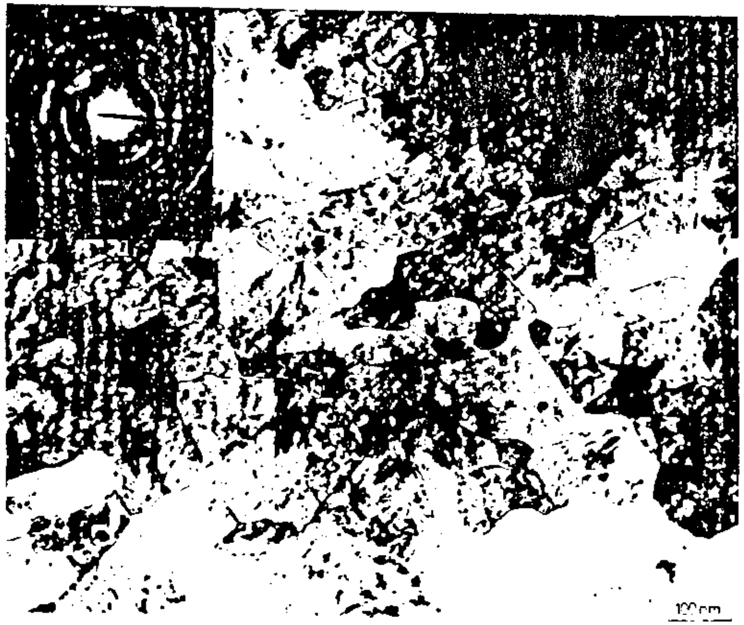

TEM

TiN on Tool Steel.

500A fine grain size

SIP coating

Why Hard

1. Fine grain size (Petch)

2. Defect Density

LECTURE 3 : SLIDE 24

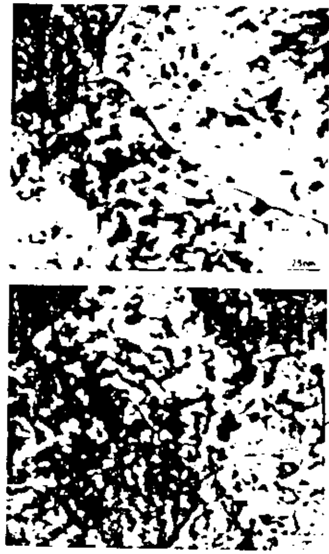

Bright field

TEM

Dark field

Now looking at defects (Dislocation loops)

(can find source of hardness.)

NB Grain Size dominates

ESTIMATED CONTRIBUTIONS TO COATING HARDNESS

System	Grain Size (Å)	Defect Density† (m^{-2})	Contribution to σ_y* ($MN\ m^{-2}$)			Calculated Hardness° ($kg\ mm^{-2}$)	Observed Hardness $H_{10\mu m}$ ($kg\ mm^{-2}$)
			Single Crystal	Grain Size	Defect Density		
TiN or M2 by SIP, -35 V substrate bias	750 [TEM]	5.6×10^{13}	7200 (60.9)	4236 (35.8)	390 (3.3)	2957	2400
TiN on stainless steel by SIP	750 [TEM]	6.6×10^{14}	7200 (60.2)	4236 (35.4)	518 (4.4)	2989	2400
TiN on M2 by ion plating	200 [Estimate]	10^{16} [Upper bound estimate]	7200 (41.4)	8202 (47.1)	2010 (11.5)	4353	4300

† From X-ray Hall plots (see Ref. 27).
* Figures in brackets are percentage contributions to total σ_y.
° Based on $H = 2.5\ \sigma_y$.

estimated f. line broadening

% contributions to total hardness due to g. size

only low % contribution

GRAIN SIZE

DOMINATES

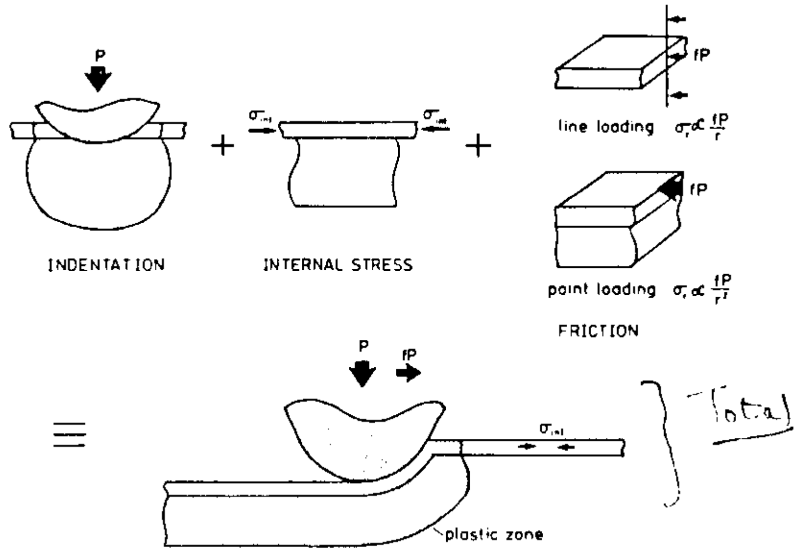

THE SCRATCH TEST

Measuring Adhesion

Try to understand

SCRATCH

TEST

LECTURE 3 : SLIDE 27

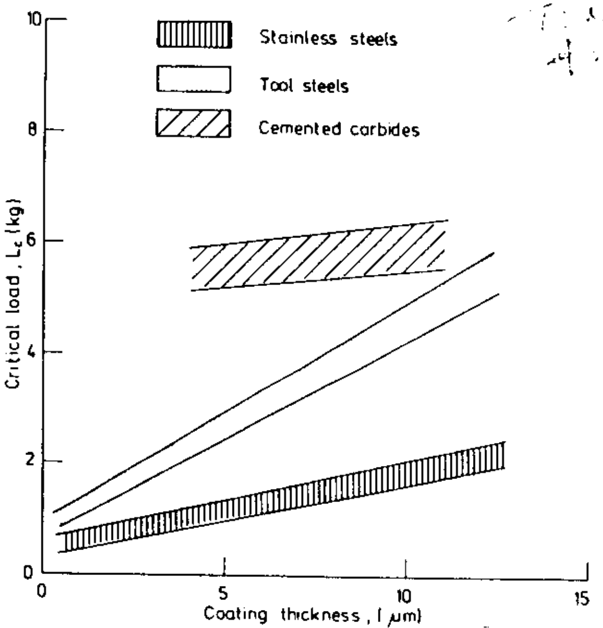

Why do we get this ranking

Stress + indentation fields

Do not yet have complete model – extension of

Hardness model to Scratch Test

should yield clarity

LECTURE 3 : SLIDE 28

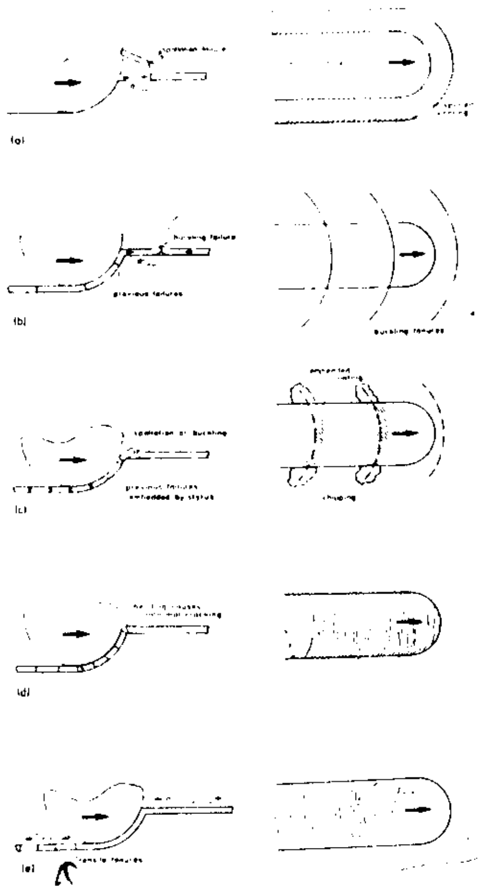

buckle failure

buckling + chipping

conformal cracking

Tensile stress cracking

Types of failure in scratch test

LECTURE 3 : SLIDE 29

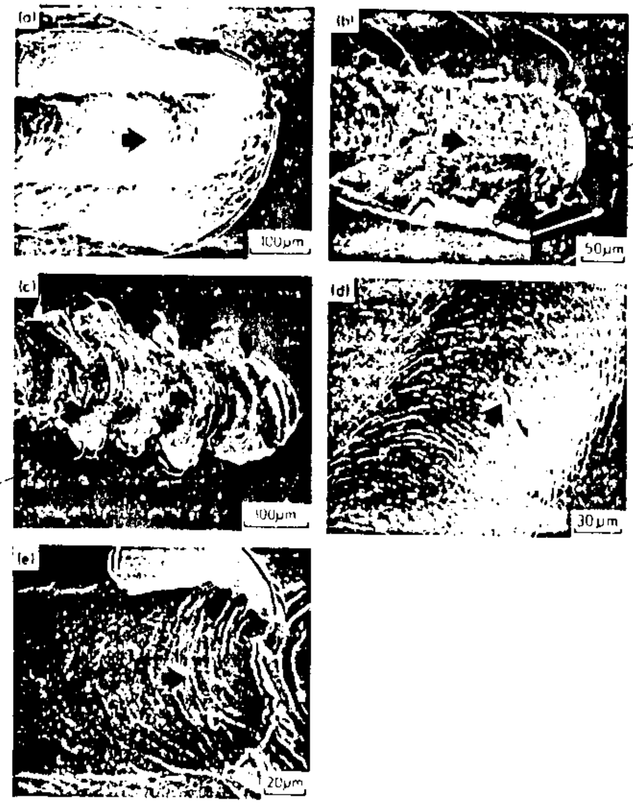

Examples of all 5 types

LECTURE 3 : SLIDE 30

INTERIM SUMMARY

A. ADVANCED PROPERTIES CAN BE CONFERRED ON INDUSTRIALLY IMPORTANT COMPONENTS BY COATINGS

B. MICROSTRUCTURE CRITICALLY AFFECTS PROPERTIES

C. IT IS POSSIBLE TO MODEL PROPERTIES E.G. HARDNESS

LECTURE 3 : SLIDE 31

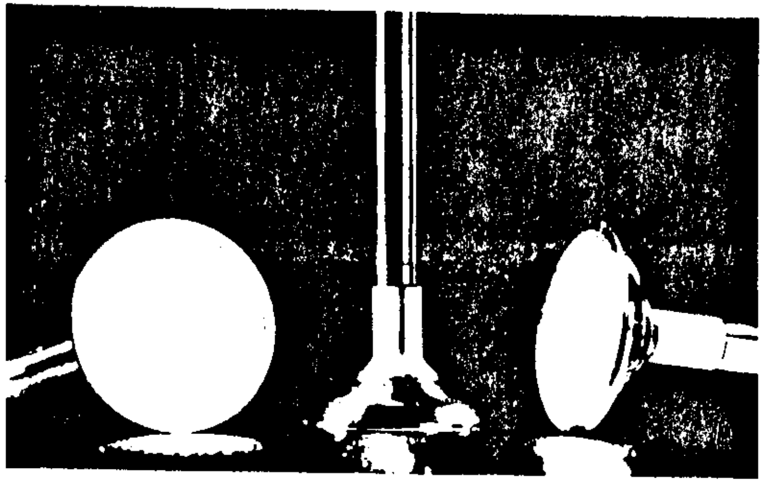

Thermal barrier

eg. Ceramics in diesel engines

ZrO_2 on exhaust valves

Property determinations on real ceramic coating and elsewhere to use

-37-

LECTURE 3 : SLIDE 32

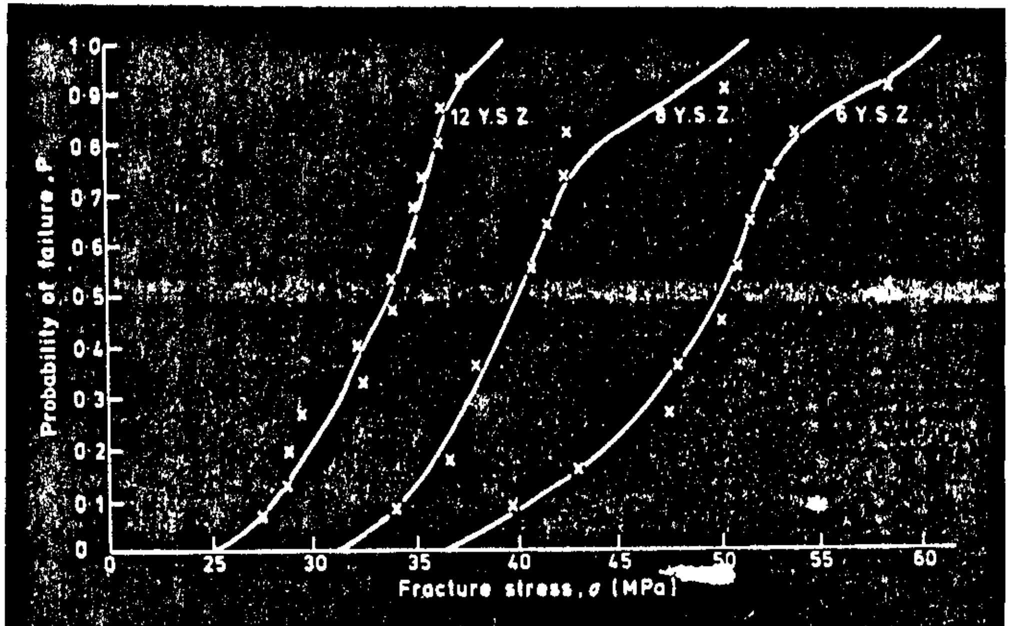

FRACTURE STRESS VERSUS ESTIMATED PROBABILITY OF FAILURE OF PLASMA SPRAYED YTTRIA STABILIZED ZIRCONIA CONTAINING DIFFERENT WEIGHT PERCENTAGES OF YTTRIA

YSZ Yttria stabilizing element

effect of

Tested ~~in~~ in laboratory on small 3 pt bending test pieces

3 POINT BEND TEST RESULTS

Material	Spraying Method	Average Fracture Stress, (MPa)	Average Youngs Modulus, E (GPa)	Weibull Modulus, m
Metco 210	Non-continuous 24g/min	29.71 ±3.28	18.38 ±2.80	10.034
Metco 210	Continuous 24g/min	33.01 ±3.95	22.79 ±4.89	9.242
Metco 210NS-1	Non-continuous 50g/min	25.66 ±3.23	14.95 ±3.66	8.741
12 Y.S.Z.	Non-continuous 50g/min	32.91 ±3.37	16.22 ±2.43	10.620
8 Y.S.Z.	Non-continuous 50g/min	40.60 ±4.57	14.79 ±1.97	9.545
6 Y.S.Z.	Non-continuous 50g/min	49.71 ±5.44	24.28 ±2.48	9.794

Importance of processing routes

NOTE

The 8 Y.S.Z. specimen was approximately half as thin as the other specimens and this will affect the comparative accuracy of the value of Youngs Modulus.

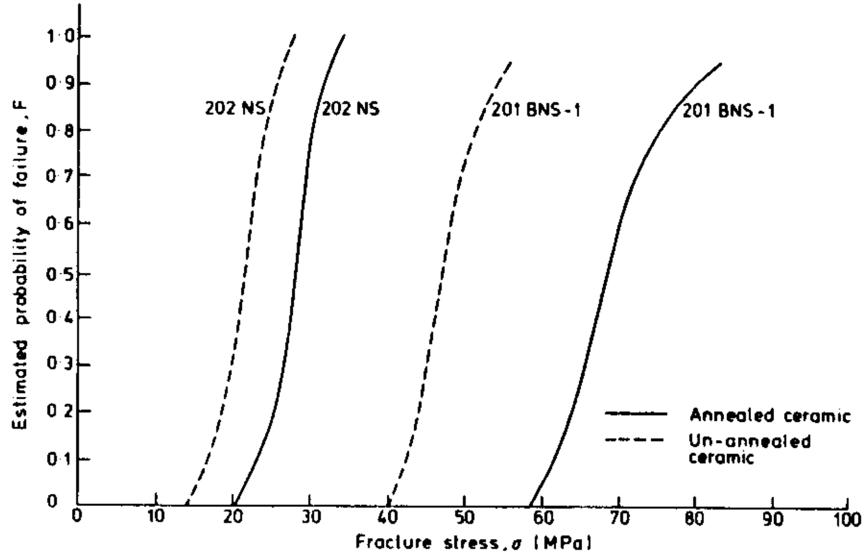

FRACTURE STRESS VERSUS ESTIMATED PROBABILITY OF FAILURE FOR TWO CERAMIC COATINGS SHOWING THE EFFECT OF ANNEALING AT 1000°C FOR 14 DAYS ALL COATINGS WERE SPRAYED CONTINUOUSLY

Huge effect of annealing

LECTURE 3 : SLIDE 35

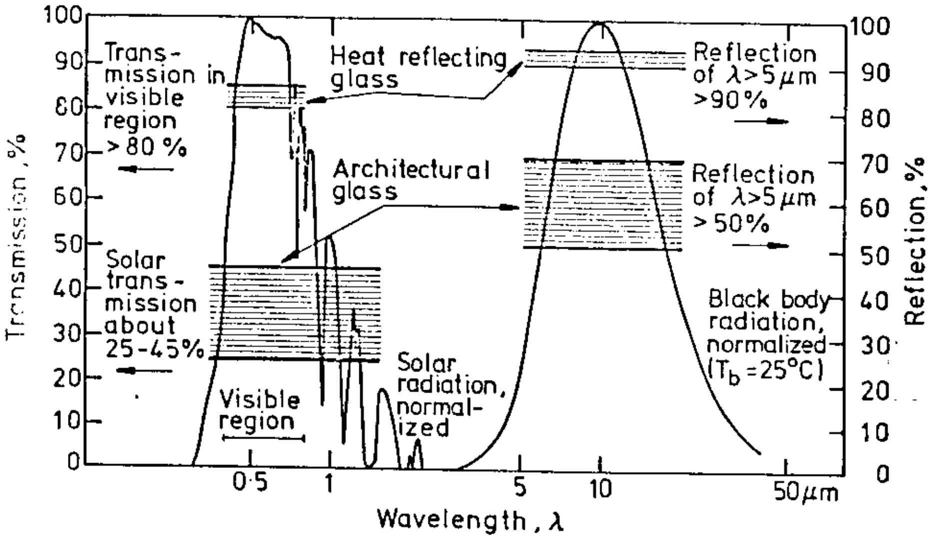

Desired physical properties of a typical heat-reflecting glass (single pane): transmission, 80%-85% in the visible region; IR reflection, more than 90%. The corresponding properties of conventional architectural glass are shown for comparison

LECTURE 3 : SLIDE 36

[illegible] ON SPE[illegible] R[illegible]SPONSE [illegible]SS.

LECTURE 3 : SLIDE 37

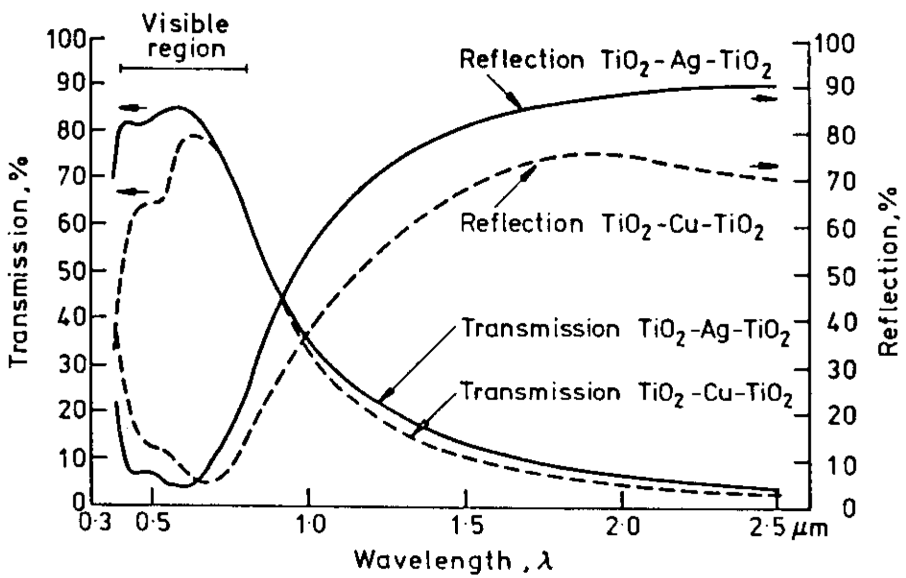

Transmission and reflection versus wavelength between 0·38 and 2·5μm for the following multilayer systems :——, TiO_2 (30 nm) / Ag (13 nm) / TiO_2 (36 nm); – – –, TiO_2 (30 nm) / Cu (13 nm) / TiO_2 (35 nm)

LECTURE 3 : SLIDE 38

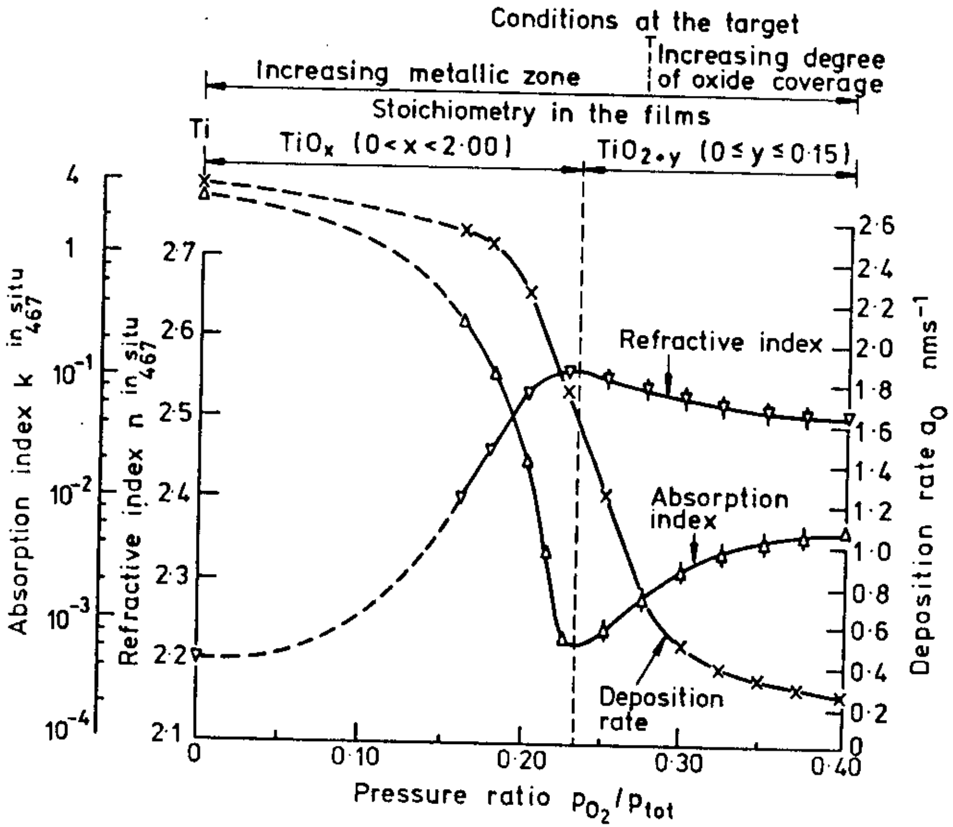

Refractive index (▽) and absorption index (Δ) of TiO_x films as well as the deposition rate (x) as functions of the pressure ratio p_{O_2}/p_{tot} used in high rate sputtering (λ = 467 nm (n and k measured in situ); $p_{Ar} = 8 \times 10^{-2}$ Pa; P = 2·5 kW; distance, 100 nm; source, PPS-5

LECTURE 3 : SLIDE 39

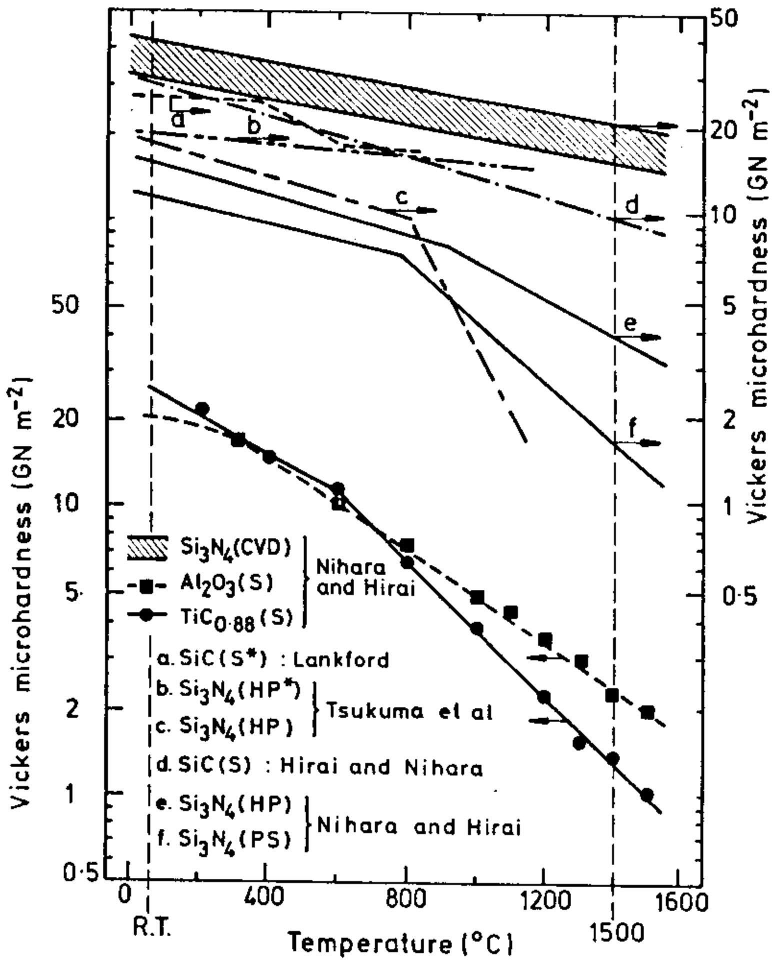

S: Single crystal, S*: Sintering, HP: Hot-pressing with additives, HP*: Hot-pressing without additives, PS: Pressureless sintering

Comparative hardness data on Si_3N_4, SiC, Al_2O_3 and TiC

LECTURE 3 : SLIDE 40

SUMMARY

A. THIN FILM PROPERTIES CAN DIFFER MARKEDLY FROM BULK PROPERTIES

B. PROPERTIES CAN BE MODELLED

C. SURFACE PROPERTIES CAN BE PRECISELY CONTROLLED E.G. FOR OPTICAL APPLICATIONS